

## Supporting Information

### Effect of separation of blocks on crystallization kinetics and phase composition of poly(butylene adipate) in multi-block thermoplastic polyurethanes

Marina A. Gorbunova,<sup>\*ab</sup> Evgenii V. Komov,<sup>b</sup> Leonid Yu. Grunin,<sup>c</sup> Mariya S. Ivanova,<sup>c</sup> Ainur F. Abukaev,<sup>d</sup> Arina M. Imamutdinova,<sup>b</sup> Dimitri A. Ivanov,<sup>abe</sup> Denis V. Anokhin,<sup>\*\*abc</sup>

<sup>a</sup> Institute for Problems of Chemical Physics Russian Academy of Sciences, Semenov Prospect 1, 142432 Chernogolovka, Russia.

<sup>\*</sup> [zav@icp.ac.ru](mailto:zav@icp.ac.ru)

<sup>b</sup> Lomonosov Moscow State University, Leninskie Gory 1, 119991 Moscow, Russia.

<sup>\*\*</sup> [deniano@yahoo.com](mailto:deniano@yahoo.com)

<sup>c</sup> Volga State University of Technology, Lenin sq. 3, 424000, Yoshkar-Ola, Russia.

<sup>d</sup> Moscow Institute of Physics and Technology, Institutskiy per. 9, 141700 Dolgoprudny, Russia

<sup>e</sup> Institut de Sciences des Matériaux de Mulhouse, CNRS UMR 7361, 15 Jean Starcky, F-68057 Mulhouse, France

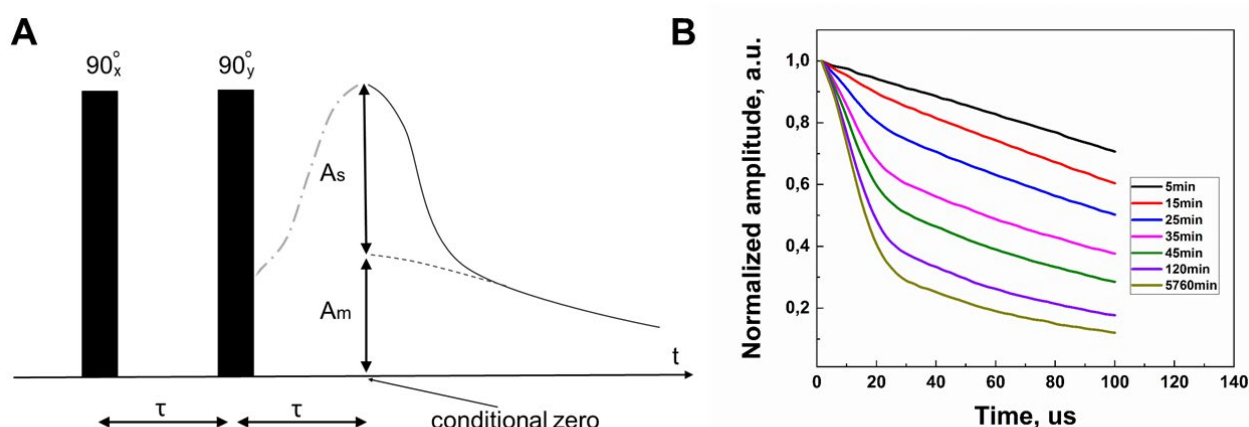


**Fig. S1** Pulse sequence diagram of the SE signal (A) and normalized SE decays of TPU-IPDI recorded in crystallization at 20 °C after cooling from 150 °C (B).

The solid-state echo decay pulse train consists of a 90° at RT pulse in the x direction followed by a 90° pulse in the y direction after a delay time  $\tau$ . Continuously increasing  $\tau$  and registering the maximum of the echo signal by  $2\tau$ , at the top of which a conditional zero is established, the decay of the transverse magnetization is recorded.

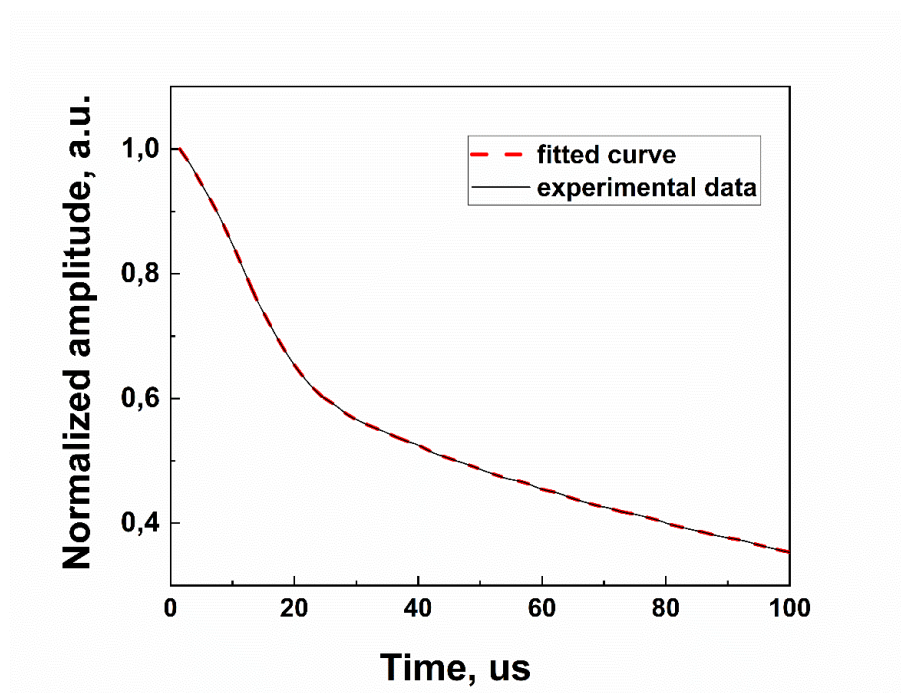


**Fig. S2** Experimental and fitted dependence of the Free Induction Decays (FID) of a two-step damping form Gaussian to exponential due to differences in the segmental mobility of the rigid and amorphous phases.

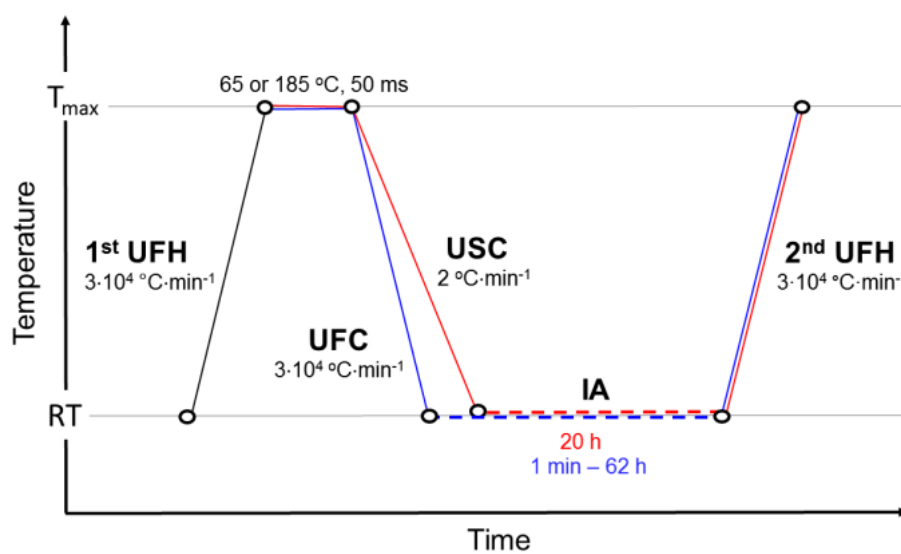


**Fig. S3** Temperature programs for nanocalorimetric measurements: Program 1 (black line), Program 2 (red lines) and Program 3 (blue lines).

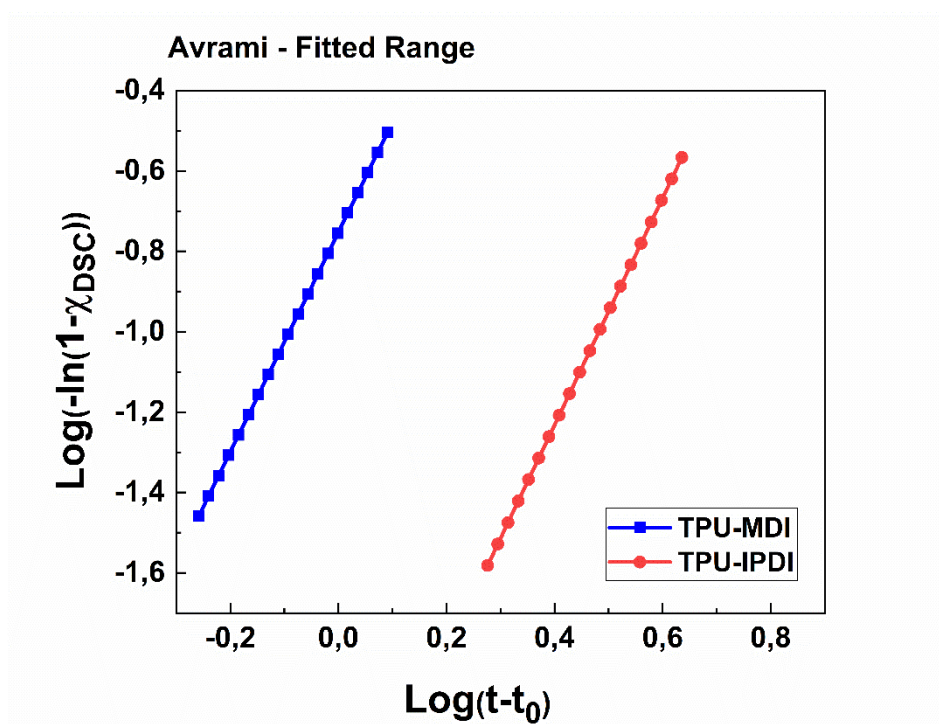


**Fig. S4** Time dependence of  $\chi_{\text{DSC}}$  in Avrami coordinates for TPU-MDI (blue curve) and TPU-IPDI (red curve).

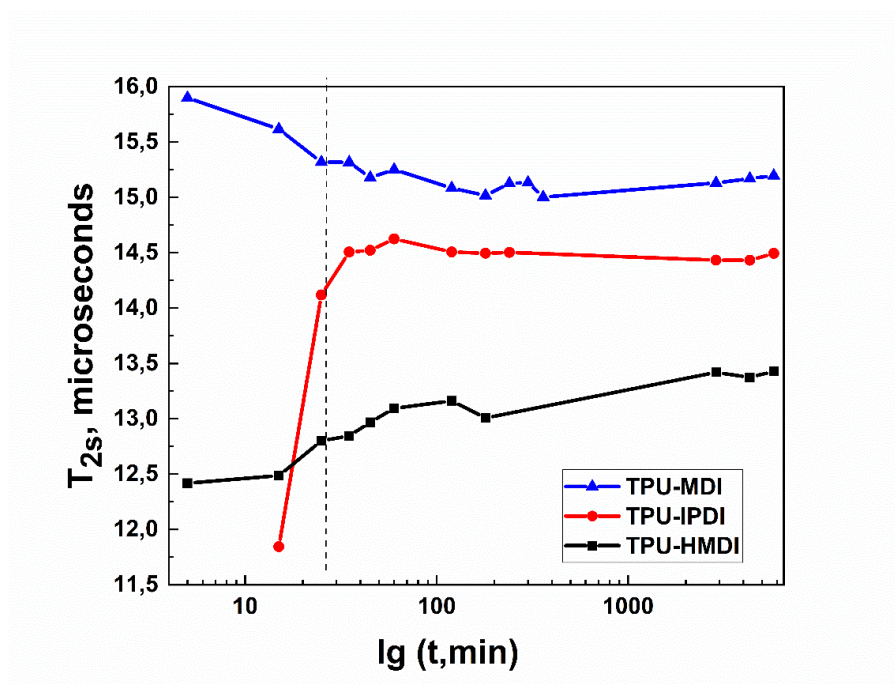


**Fig. S5** Changes in the spin-spin relaxation time  $T_{2s}$  during crystallization at 20 °C after cooling from 150 °C.

Normally, the general trend in relaxation time of a rigid fraction with cooling and crystallizing should show the decrease of  $T_{2s}$ . For the sample TPU-HMDI we observe definitely reversed behavior that can be explained by more intensive magnetization exchange between crystals and amorphous regions due to presence of in intermediate mesophase.

**Table S1** Main frequencies and assignments of FTIR bands to crystal phases of PBA oligodiol.

Main assignment	Wavenumber, $\text{cm}^{-1}$	Phase	Wavenumber, $\text{cm}^{-1}$	Phase	Wavenumber, $\text{cm}^{-1}$	Phase
	20 °C/min		2 °C/min		storage at RT	
$\gamma$ CH <sub>2</sub>	911	$\beta$	908	$\alpha$	908	$\alpha$
$\gamma$ CH <sub>2</sub>	930	$\beta$	-	$\alpha$	-	$\alpha$
$\gamma$ CH <sub>2</sub>	958	$\beta$	957	$\alpha$	957	$\alpha$
$\sigma_s$ CH <sub>2</sub>	1371	$\beta$	1368	$\alpha$	1368	$\alpha$
$\sigma_{as}$ CH <sub>2</sub>	1401	$\beta$	1398	$\alpha$	1398	$\alpha$
$\delta_s$ CH <sub>2</sub>	1416	$\beta$	1418	$\alpha$	1418	$\alpha$
$\delta_{as}$ CH <sub>2</sub>	1464	$\beta$	1461	$\alpha$	1461	$\alpha$
$\nu_{as}$ C-O-C	1258	$\beta$	1257	$\alpha$	1257	$\alpha$
$\nu_s$ C-O	1162	$\beta$	1160	$\alpha$	1160	$\alpha$

Thus, it has been established that upon 20 °C/min cooling, the pure  $\beta$ -form crystallizes, while upon 2 °C/min cooling, the pure  $\alpha$ -form crystallizes («fresh»). Storage («old») of PBA at RT leads to the formation of the  $\alpha$ -phase.

**Table S2** Main frequencies and assignments of FTIR bands to crystal phases of PBA in TPUs.

Main assignment	wavenumber, $\text{cm}^{-1}$	phase	wavenumber, $\text{cm}^{-1}$	phase	wavenumber, $\text{cm}^{-1}$	phase
	TPU-MDI		TPU-IPDI		TPU-HMDI	
2 °C/min after 65 °C						
$\gamma$ CH <sub>2</sub>	910	$\alpha+\beta$	910	$\alpha+\beta$	909	$\alpha+\beta$
$\gamma$ CH <sub>2</sub>	930	$\alpha+\beta$	930	-	930	$\alpha+\beta$
$\gamma$ CH <sub>2</sub>	959	$\beta$	960	$\beta$	959	$\beta$
$\sigma_s$ CH <sub>2</sub>	1369	$\alpha+\beta$	1369	$\alpha+\beta$	1368	$\alpha$
$\sigma_{as}$ CH <sub>2</sub>	1397	$\alpha$	1398	$\alpha$	1396	$\alpha$
$\delta_s$ CH <sub>2</sub>	1415	$\alpha+\beta$	1418	$\alpha$	1417	$\alpha$
$\delta_{as}$ CH <sub>2</sub>	1462	$\alpha$	1461	$\alpha$	1463	$\alpha+\beta$
20 °C/min after 150 °C						
$\gamma$ CH <sub>2</sub>	910	$\alpha+\beta$	910	$\alpha+\beta$	910	$\alpha+\beta$
$\gamma$ CH <sub>2</sub>	930	$\alpha+\beta$	930	$\alpha+\beta$	930	-
$\gamma$ CH <sub>2</sub>	959	$\beta$	958	$\beta$	958	$\beta$
$\sigma_s$ CH <sub>2</sub>	1369	$\alpha+\beta$	1368	$\alpha$	1368	$\alpha$
$\sigma_{as}$ CH <sub>2</sub>	1397	$\alpha$	1398	$\alpha$	1396	$\alpha$
$\delta_s$ CH <sub>2</sub>	1414	$\beta$	1418	$\alpha$	1417	$\alpha$
$\delta_{as}$ CH <sub>2</sub>	1461	$\alpha+\beta$	1461	$\alpha$	1461	$\alpha$
20 °C/min after 185 °C						
$\gamma$ CH <sub>2</sub>	-	-	-	-	909	$\alpha+\beta$
$\gamma$ CH <sub>2</sub>	-	-	-	-	930	$\alpha+\beta$
$\gamma$ CH <sub>2</sub>	-	-	-	-	959	$\beta$
$\sigma_s$ CH <sub>2</sub>	-	-	-	-	1369	$\alpha+\beta$
$\sigma_{as}$ CH <sub>2</sub>	-	-	-	-	1398	$\alpha+\beta$
$\delta_s$ CH <sub>2</sub>	-	-	-	-	1417	$\alpha$

$\gamma$ CH <sub>2</sub>	-	-	-	-	1463	$\beta$
--------------------------	---	---	---	---	------	---------

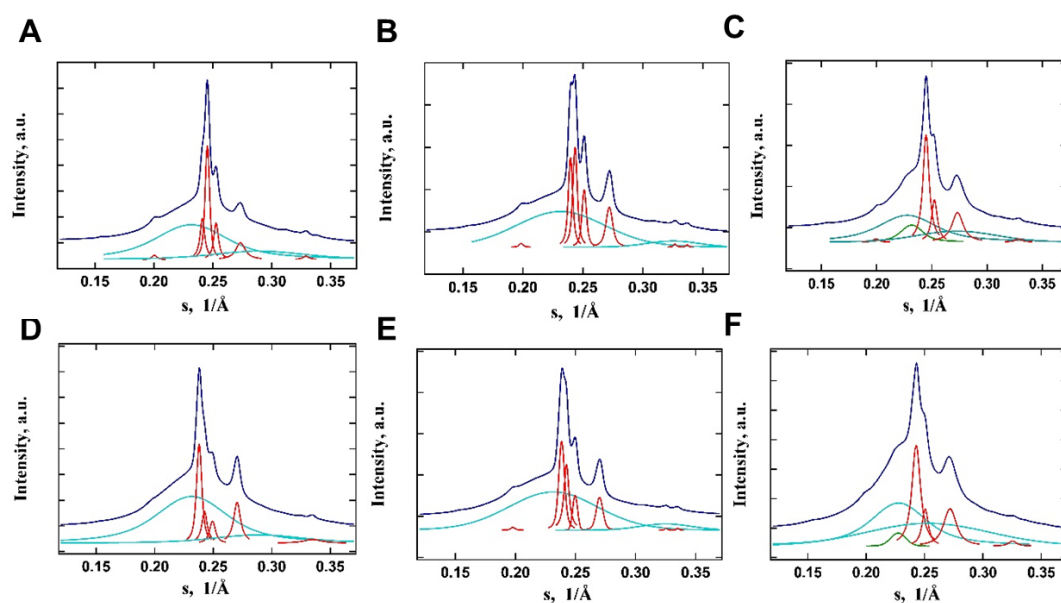


**Fig. S6** Fitting with set of Gaussians of WAXS patterns of TPU-MDI (A, D), TPU-IPDI (B, E) and TPU-HMDI (C, F) after long storage (A-C) and after crystallization from 150 °C for 20 hours at RT (D, F). Red, cyan and green curves indicate crystalline, amorphous and mesophase peaks, respectively.

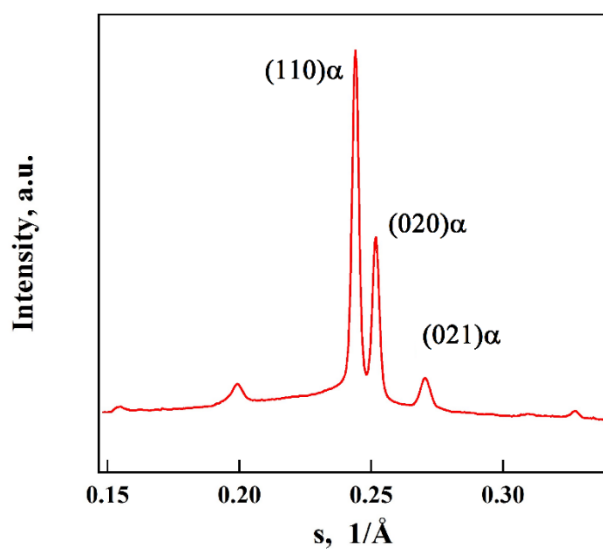


**Fig. S7** WAXS diffractogram of PBA oligodiols (only  $\alpha$  modification).

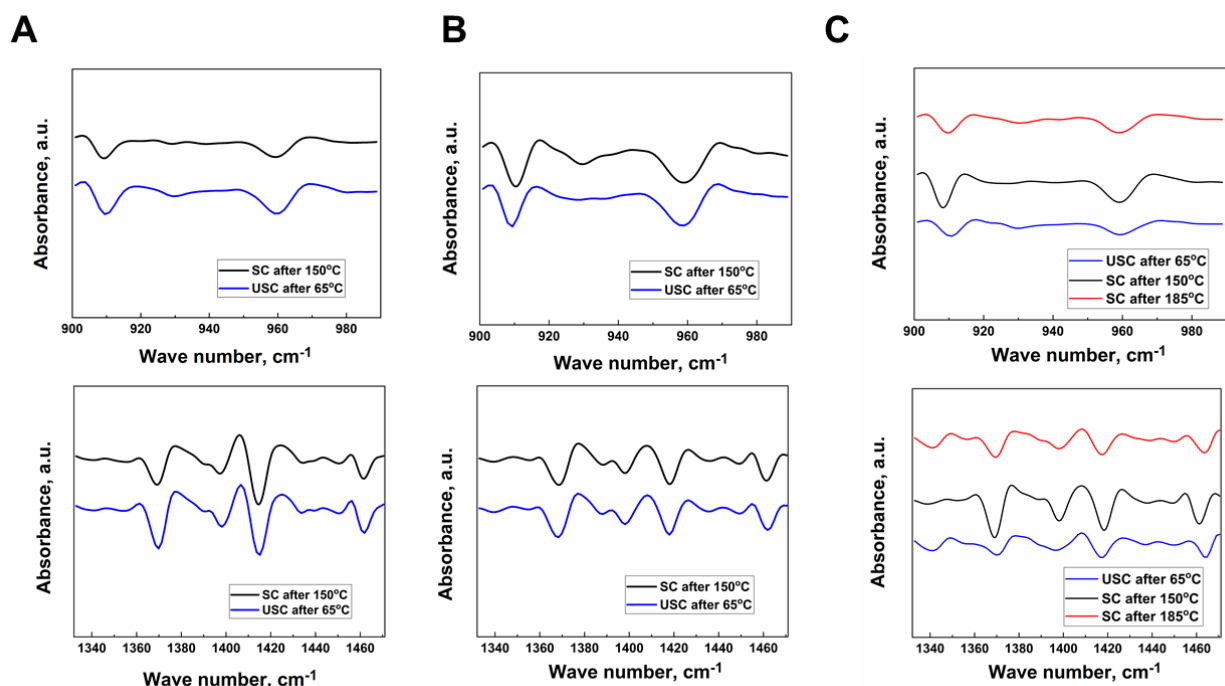


**Fig. S8** Second derivatives of the IR spectra of the TPU series for TPU-MDI (A), TPU-IPDI (B) and TPU-HMDI (C), differing in the hard block structure and crystallized under different cooling conditions.

**Table S3** Effect of crystallization conditions on the phase composition of PBA for different TPUs taken at the same time interval after crystallization

Sample preparation conditions	Cooling	Rate, °C/min	T <sub>max</sub> heat, °C	FSC*	FTIR	WAXS
PBA						
stored at RT	-			$\alpha^{**}$	$\alpha$	$\alpha$
recrystallized at RT	UFC	30000	185	$\beta$	-	-
	SC	20	65	-	$\beta$	-
	USC	2	65	-	$\alpha$	-
TPU-MDI						
stored at RT	-			$\alpha+\beta^{**}$	$\alpha+\beta$	$\alpha+\beta$
recrystallized at RT	UFC	30000	185	$\alpha$	-	-
	USC	2	185	$\alpha+\beta$	-	-
	SC	20	150	-	$\alpha+\beta$	$\alpha+\beta$
	USC	2	65	-	$\alpha+\beta$	-
TPU-IPDI						
stored at RT	-			$\alpha+\beta^{**}$	$\alpha+\beta$	$\alpha+\beta$
recrystallized at RT	UFC	30000	185	$\alpha$	-	-
	USC	2	185	$\alpha+\beta$	-	-
	SC	20	150	-	$\alpha+\beta$	$\alpha+\beta$
	USC	2	65	-	$\alpha+\beta$	-

TPU-HMDI						
stored at RT	-			$\alpha^{**}$	$\alpha$	$\alpha$
recrystallized at RT	UFC	30000	185	$\alpha+\beta$	-	-
	SC	20	185	-	$\alpha+\beta$	-
	USC	2	185	$\alpha$	-	-
	SC	20	150	-	$\alpha$	$\alpha$
	UFC	30000	65	$\alpha$	-	-
	USC	2	65	$\alpha$	$>\alpha$	-

\*UFH/UFC – ultra-fast heating/cooling with rate of 30 000 °C/min

\*\*heating of the initial sample from RT to 185 °C

SC – slow cooling with rate of 20 °C/min

USC – ultra-slow cooling with rate of 2 °C/min

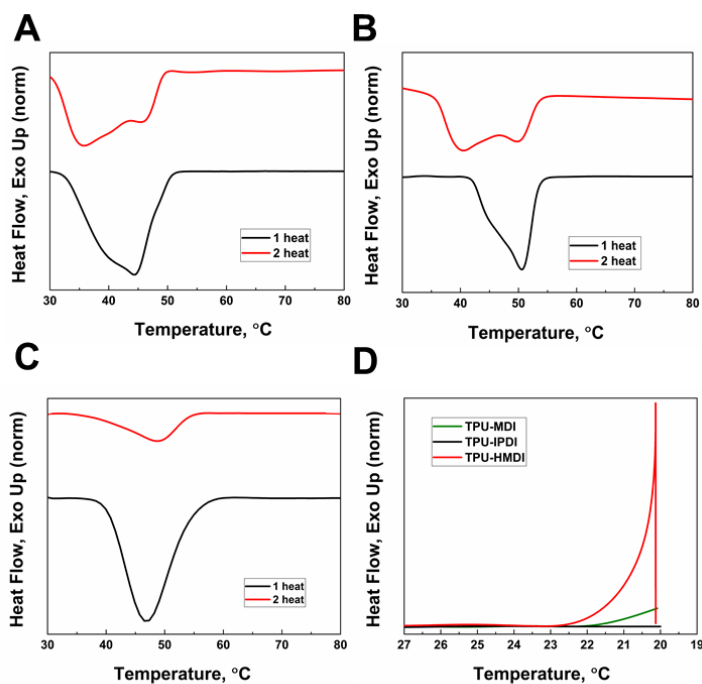


**Fig. S9** DSC heating curves up to 150 °C of the initial films (1st heating, black curves) and after 30-min crystallization at 20 °C (2nd heating, red curves) for TPU-MDI (A), TPU-IPDI (B), TPU-HMDI (C) and 1<sup>st</sup> cooling curves (D).

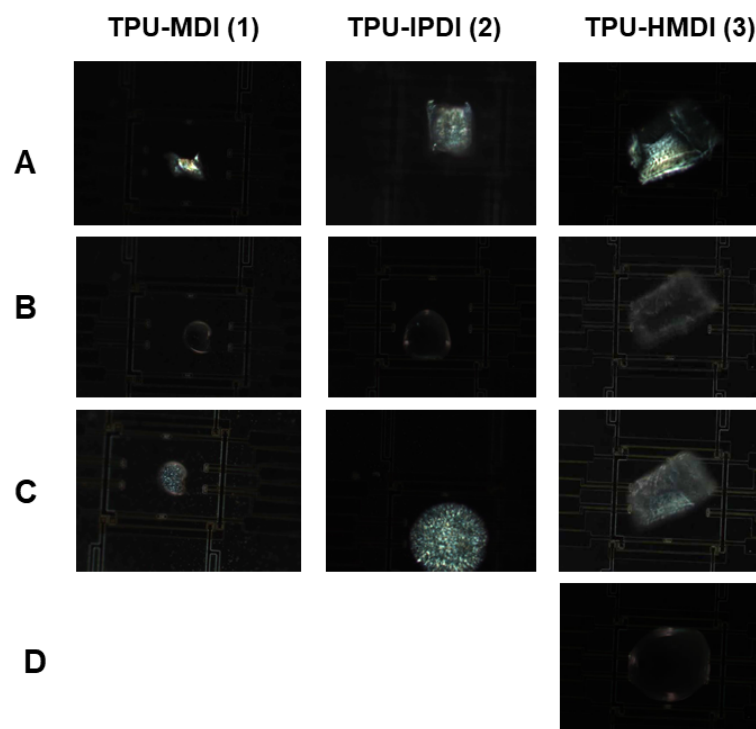


**Fig. S10** Micrographs of TPU microparticles in polarized light.

For TPU-IPDI and TPU-MDI: particle linear sizes are about 75x75 and 40x30 microns, respectively. Before the 1<sup>st</sup> heating (A); after the 1<sup>st</sup> heating, at 185 °C (B); after 20 hour annealing at RT, right before the 2<sup>nd</sup> heating (C). For TPU-HMDI: particle linear sizes are about 100x70 microns. Before the 1<sup>st</sup> heating (A); after the 1<sup>st</sup> heating, at 65 °C (B); after 20 hour annealing at RT, just before the 2<sup>nd</sup> heating to 185 °C (C); just after the 2<sup>nd</sup> heating, at 185 °C (D).